Activation, Transportation and Reaction of Alkyl Radicals on a Si(111)-B Surface by a STM tip

*Elie GEAGEA,[1] Judicaël JEANNOUTOT,[1] Frank PALMINO,[1] Alain ROCHEFORT, [2] and Frédéric CHÉRIOUX *,[1]*

[1] Université de Franche-Comté, FEMTO-ST, CNRS, 15B avenue des Montboucons, F-25030 BESANÇON, France.

[2] Département de génie physique, Polytechnique Montréal, Montréal (Qué), Canada, H3C 3A7.

KEYWORDS. Scanning Tunneling Microscopy, Organic Radical, Silicon, DFT.

ABSTRACT. On-surface chemistry is a powerful method to fabricate organic nanostructures with high precision onto different kinds of surfaces. On more inert surfaces, the lack of reactivity of the underlying substrate can be circumvented by using the electrons from a scanning tunnelling microscope (STM) tip, as a stimulus, to produce the reactants of a targeted reaction. Here, another role for the STM tip is exploited in the fabrication of organic nanostructures. The STM tip is first used as a source of stimulating electrons to generate organic radicals on a Si(111)√3x√3R30°-B surface. Then, the STM tip acts as a conveyor to transfer radicals among different interfaces, for finally creating new hybrid organic-inorganic interfaces. Our approach enables new alternatives to initiate, control and provide radicals into oligomerization reactions with tunnelling electrons, and to fabricate nanostructure with a molecular precision.

INTRODUCTION

On-surface synthesis (OSS) constitutes a rapidly growing field that continuously attracts the attention of the scientific community due to its fundamental role in the development of single-layered polymers coatings. Indeed, OSS remains one of the most powerful bottom-up direction for the fabrication of atomically precise nanoarchitectures.[1,2,3,4,5,6] The OSS approach consists in the formation of covalent coupling among molecular entities that are adsorbed on a well-defined surface. Metallic surfaces are by far the most frequently used substrates, semiconducting and insulating surfaces are rarely investigated. Two-dimensional confinement of reagents imposed by the surface topology can give an access to entirely new reactional pathways as compared to solution reactions. Furthermore, since OSS is usually performed without solvent, this significantly enlarges the choice of precursors that can be used, even insoluble compounds. OSS of π-conjugated (e.g., unsaturated) nanostructures were widely studied due to their promising conducting properties for applications in optics, spintronics, electronics, etc.[2,7] However, the synthesis of saturated molecules on surfaces, such as alkanes, is still of high interest. In early works, long alkyls molecular chains were deposited on a graphite surface[8,9] to promote the formation of large-scale 2D-self-assemblies,[10,11] but also on a silicon surface to produce molecular electronic switch.[12] More recently, alkanes were used in an OSS on metal surfaces via C-H bond activation to guide 1D-polymerization,[13,14] and as a decoupling layer to promote 2D photo-induced polymerization.[15] On a semiconducting surface in ultra-high vacuum (UHV) conditions, we have reported in a previous work, alkane oligomerization by using electrons from the STM tip as external stimulus.[16] In this case, oligomerization reaction did not occur where the alkyl radicals were produced, but on a free region of the same underlying silicon surface by using the STM tip to store and transfer the generated active radicals. Although the participation of organic radicals in

such on-surface chemistry reactions was oftenly mentioned in the literature,[5,17] only a small number of papers have shown a direct evidence for the presence of organic radicals on a surface using scanning probe microscopies.[18] Hence, the presence of radicals is generally assumed when the nature of final surface species can only be explained by a reaction of alkyl radicals with surface atoms.[16] Atoms or molecules manipulation by a STM tip was demonstrated at a very early stage of the STM invention to create artificial nanostructures on a surface.[19] Subsequently, STM tip has been used to induce on-surface chemical reaction, through a series of localized excitation and manipulation of adsorbed molecules.[19,20] However, all these reactions were induced by a local excitation of molecules adsorbed on a surface without transferring reactive species among different interfaces. The present work highlights a new role of the STM tip in OSS: we demonstrate that an STM tip can generate and transport reactive alkyl radicals from one surface and then deposit them on a different surface. More precisely, we produced alkyl radicals from a first supramolecular network that was built on a given substrate, transported the reactive alkyls into the nanopores of a second supramolecular network, grown on a different surface, simply by using the STM tip. This work was achieved by means of STM on a silicon surface at 110 K, and supported by DFT simulations. This unprecedented method of functionalization leads to multi-functional nanostructures, which are only accessible by this double activation/transport process of active species.

METHODS

Molecules

The two molecules used in this article have been synthesized according to the procedures described in the literature.[16,21]

Surface preparation and STM experiments

The substrate was a silicon wafer highly doped with boron (B) atoms ($\rho = 10^{-3}$ Ω.cm). Inside the UHV chamber, we carefully degassed the sample by limiting the pressure excess to 10^{-10} mbar range, up to 1073 K. Then, the sample was flashed several times, by increasing temperature up to 1423 K to allow the elimination of any impurities, and to remove a few top atomic layers. The following step consisted of a thermal annealing at 1123 K for 1 hour, where the B atoms migrate to occupy around one third atomic sites of the layer under the silicon adatoms of the surface. This heat treatment leads to the reconstruction Si(111)-B √3x√3 R30° or simply Si(111)-B (see Figure S1).[22] The obtention of the Si(111)-B surface reconstruction as well as its cleanliness was verified by STM. Cleaning procedure was performed until large scale STM images with a minimal amount of defects and free of impurities (Figure S1) were obtained. On this clean surface, molecules were deposited from quartz crucibles while sample was placed in front of the crucible and held at room temperature (RT). Finally, the sample was transferred to the STM head and cooled down to 110 K before acquiring images in a current constant mode. Sublimation temperature was 438 K and 463 K, for respectively the PDB-OC10 (first supramolecular assembly) and TCNBB (second assembly with nanopores) molecules.

DFT simulations

The DFT calculations were performed using the Siesta package (version 4.1.5),[23,24] within the vdW-DF2 functional limit.[25] The Si(111)-B substrate was modeled by a large unit cell of 783 atoms (588 Si, 49 B, 146 H) terminated with hydrogen atoms to avoid the presence of Si dangling bonds. Prior to any molecular adsorption, the three top layers including the B atoms of the Si(111)-B substrate were fully optimized (max forces tolerance < 0.02 eV/Å, total energy variation < 10^{-5}

eV). The adsorption of the TCNBB network on Si(111)-B was modeled by considering six TCNBB molecules (270 C, 18 N, 162 H) on the optimized Si(111)-B substrate, the TCNBB molecular arrangement was fully optimized (max forces tolerance < 0.02 eV/Å, total energy variation < 10^{-5} eV) while the Si(111)-B substrate was kept fixed. We then used that optimized TCNBB network on Si(111)-B (a 1233 atoms unit cell), and kept it frozen during the subsequent adsorption and optimization of C_{10} and C_{20} molecular fragments (max forces tolerance < 0.02 eV/Å, total energy variation < 10^{-5} eV) on the TCNBB/Si(111)-B network. All optimizations were performed at Γ−point (*k*-point mesh of 1x1x1), and the properties were calculated with a 3x3x1 *k*-point grid. The Bader charge analysis was performed with the Bader code developed by the Henkelman group.[26] STM simulations images were evaluated at Tersoff-Hamann (TH) level of theory,[27] the topology images were obtained at constant current mode.

RESULTS and DISCUSSION

STM experiments

Si(111)–B has been chosen as a semiconducting surface due to the saturation of the dangling bonds of silicon adatoms by B atoms underneath, which offers a unique platform for the engineering of molecular patterns.[28] We have chosen two molecules for this study. The first one is an aryl alkyl ether derivative because (i) this type of molecule can be cleaved via one-electron reduction process to undergo the formation of phenoxide anions and alkyl radicals[29,30] and (ii) these molecules aim to self-assemble on surfaces.[16] The second type of molecule is a star-shaped molecule that forms nanoporous supramolecular networks onto surfaces.[31]

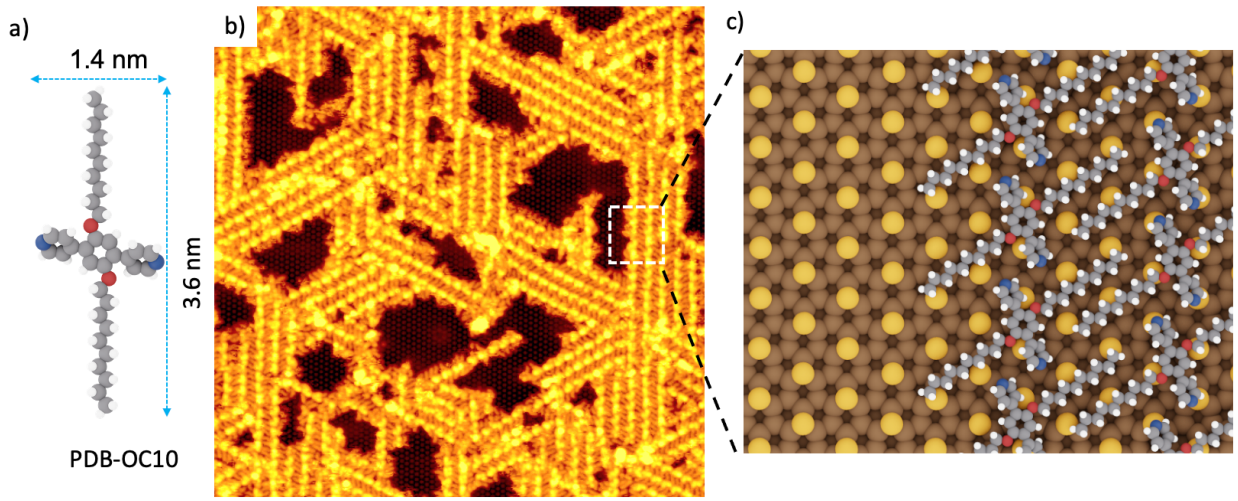

Figure 1. a) Structural model of 1,4-di(4',4"-pyridyl)-2,5-bis(decyloxy)benzene (PDB-OC10) molecule. b) Large-scale high-resolution STM image (60 nm x 60 nm, V_s = -1.3 V, I_t = 7 pA, T = 110 K) of PDB-OC10 molecules self-assembled on a Si(111)-B surface. c) Proposed molecular model of the PDB-OC10 adlayer shown in b). Nitrogen atoms: blue, Oxygen atoms: red, Carbon atoms: grey, Hydrogen atoms: white, Silicon adatoms: yellow, bulk Silicon atoms: light brown.

1,4-di(4',4"-pyridyl)-2,5-bis(decyloxy)benzene (PDB-OC10) molecule is made of a central phenyl core substituted with two lateral ether alkyl chains (Figure 1a) with 10 carbon atoms (C_{10}) and with two pyridyl moieties. The total alkyl side-chain length in PDB-OC10 is 3.6 nm while the length of the aromatic core is 1.4 nm (Figure 1a). PDB-OC10 molecules were deposited by thermal sublimation under UHV conditions on a Si(111)-B substrate maintained at RT. A typical large-scale STM image recorded at 110 K is shown in Figure 1b (corresponding zoom in Figure S2). As we previously demonstrated, [16,32,33] this image corresponds to the formation of a supramolecular network of PDB-OC10 molecules, as illustrated in the model in Figure 1c. This supramolecular network is stabilized by molecule-molecule interactions, mostly due to interdigitation of C_{10} alkyl

chains of two PDB-OC10 molecules involved in two adjacent lines and by molecule-surface interactions, mostly due to the N – Si adatoms interactions.

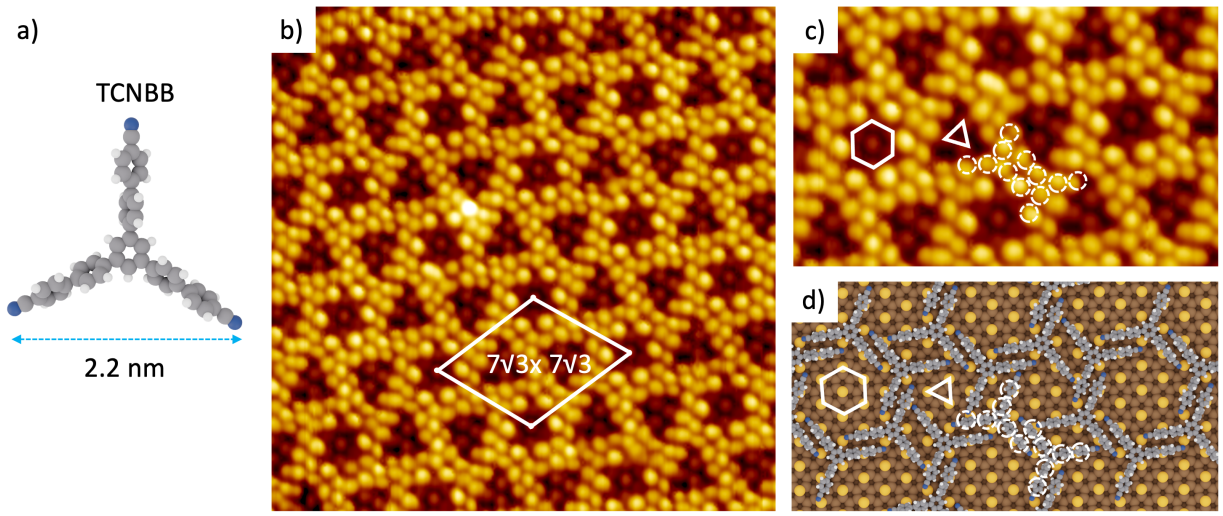

Figure 2. a) Structural model of 1,3,5-tri(4”-cyano-4,4’-biphenyl)benzene (TCNBB) molecule. b) High-resolution STM image (20 nm x 20 nm, V_s = 2.5 V, I_t = 10 pA, T = 110 K) of TCNBB molecules self-assembled on a Si(111)-B surface. c) Zoom area of the network shown in b) (12 nm x7 nm). Two types of nanopores were identified: the first one is constituted by seven Si adatoms in a hexagon-centered shape and the second one is constituted by three Si adatoms that give a triangle, highlighted by white hexagon and triangle respectively. Six bright protrusions (surrounded by dashed circles) are attributed to a single TCNBB molecule. d) Proposed molecular model of the TCNBB adlayer shown in c). Same color scheme as used in Figure 1.

1,3,5-tri(4”-cyano-4,4’-biphenyl)benzene molecule (TCNBB) is based on benzene central ring substituted at the 1, 3, and 5 positions by a biphenyl ended by a CN group (Figure 2a).[21] This molecule was deposited on a Si(111)-B substrate at RT by thermal sublimation under UHV conditions. With STM, we observed a nanoporous network, based on hexagonal nanopores surrounded by six triangular nanopores, oriented at 60° from one to the other (Figure 2b). In

hexagonal nanopores, seven protrusions are observed while for each triangular nanopores, only three protrusions can be seen (Figure 2c). Based on these experimental findings, the corresponding supramolecular model is described in Figure 2d. TCNBB molecule appears as six bright protrusions (white dashed circles in Figure 2d), while each protrusion included in nanopores is attributed to a silicon adatom. This model is also similar to the one observed for the bromine-ended molecule[34] instead of cyano-ended.

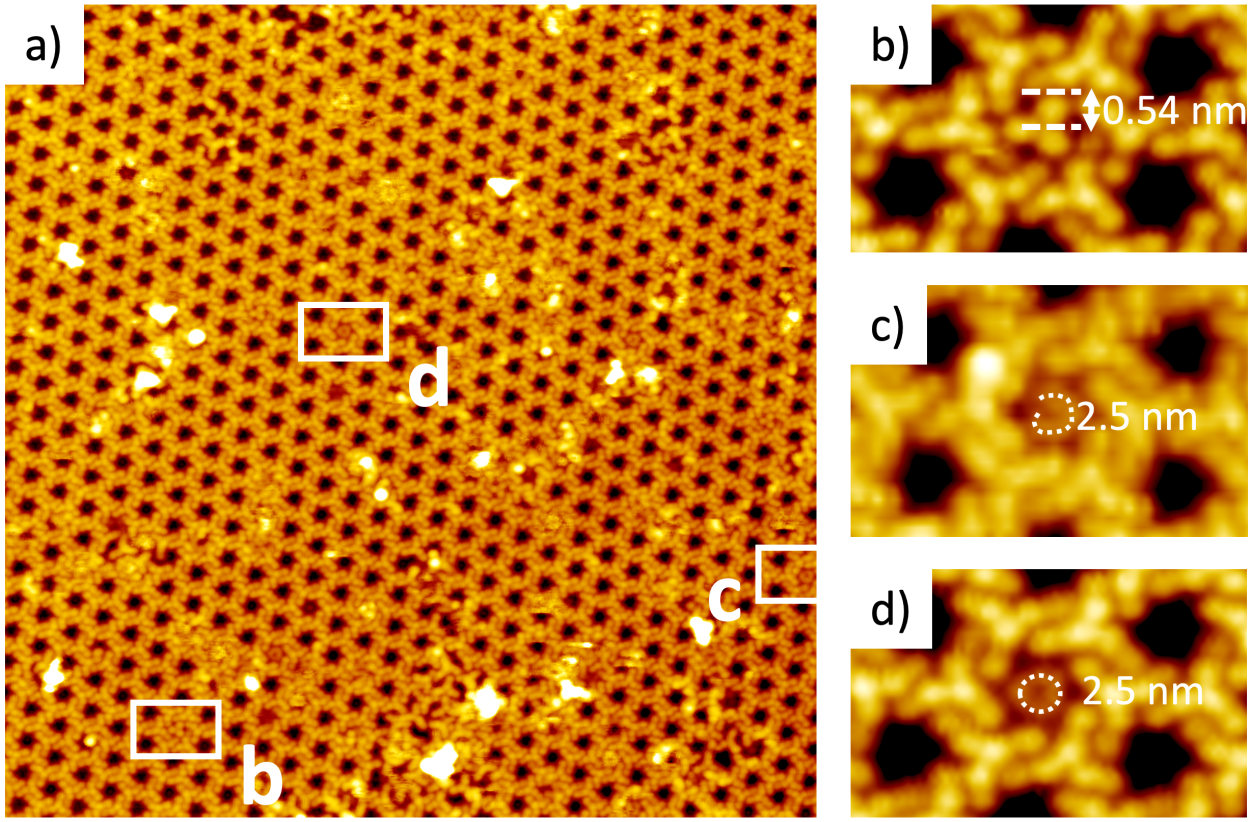

Figure 3. a) High resolution STM image (70 nm x 70 nm, V_s = -2.5 V, I_t = 10 pA, T = 110 K) of TCNBB supramolecular network on a Si(111)-B surface obtained after a scanning with a tip used for a previous scanning of the PDB-OC10 adlayer. Some nanopores are filled with new structures highlighted by white rectangles (8 nm x 5 nm) quoted b-d. b) Triangular nanopore filled with three bright disjoint protrusions, each one having a diameter of 0.54 nm. c) Hexagonal nanopore filled

with opened ring-like structure with a length of 2.5 nm. d) Hexagonal nanopore filled with closed ring-like structure with a length of 2.5 nm.

Here, we aim to highlight the role of the STM tip in the transfer of alkyl radicals from one surface to another one. To achieve final structures, the alkyl radicals were firstly produced through the dissociation of PDB-OC10 molecules. According to our previous results,[16] the C_{10} alkyl radicals were generated by dissociating a given number of PDB-OC10 molecules through scanning an area containing self-assembled PDB-OC10 molecules on the Si(111)-B surface at -4.5 V and 750 pA. Then, we checked that all cross-shaped features associated to PDB-OC10 molecules have disappeared from the scanned area (see Figure S3). The STM tip used for the scanning the first PDB-OC10 network was also used to scan the second TCNBB supramolecular network. The TCNBB network was independently prepared onto a different Si(111)-B substrate, and stored in the STM chamber. The TCNBB supramolecular network was scanned at V_s = -2.5 V and I_t = 10 pA at 110 K for 40 minutes. After scanning, we observed that 1.7% of the entire amount of nanopores were filled by different nanostructures (surrounded by white rectangles in Figure 3) which appear slightly darker than the TCNBB molecules. Three types of nanostructures were observed in nanopores. Within 0.9 % of triangular nanopores, three disjoint protrusions, each one having a diameter of 0.54 ± 0.05 nm, are observed (Figure 3b). In the case of hexagonal nanopores, 3.4 % of them are filled with a closed ring-like structure of a length of 2.5 ± 0.1 nm (Figure 3c) while 0.9% of hexagonal nanopores are filled with opened ring-like structure (Figure 3d).

Discussion and DFT simulations

To fully understand the nature of the new confined features observed in the STM images of nanopores, we have carefully surveyed the literature. We found that very similar types of confined

features have been recently observed after an exposure of 300 L of propylene on a clean Ni(111) surface at room temperature.[35] The authors corroborated their experimental observations by DFT simulations. The authors attributed the disjoint protrusions of short alkyl chain grafted onto Ni surface atoms, and open-ring and closed-ring shaped to acyclic and cyclic alkane chains adsorbed in the plane of the Ni(111) surface. Based on this work, we can then propose the three following models to relate our STM images.

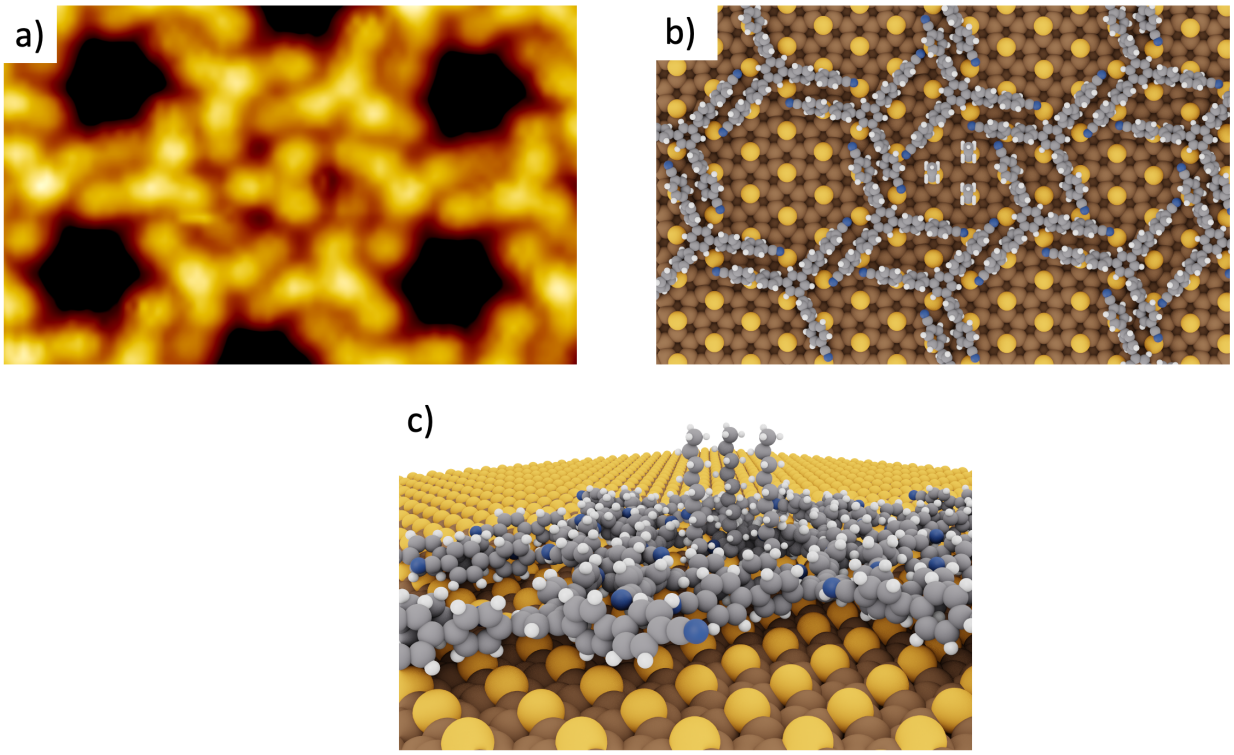

Figure 4. a) High-resolution STM image (8 nm x 5 nm, V_s = -2.5 V, I_t = 10 pA, T = 110 K) of a triangular nanopore of TCNBB supramolecular network on a Si(111)-B surface including three bright protrusions. b) Proposed molecular model of the triangular nanopore filled with three bright protrusions shown in a). Each bright protrusion is attributed to a single decyl chain grafted onto a surface Si adatom. c) side-view of b).

We attribute each disjoint bright protrusion observed in triangular nanopores of the TCBNN supramolecular network to a C_{10} alkyl chain grafted on one of the three Si adatoms present in the nanopore (Figures 4b-c).

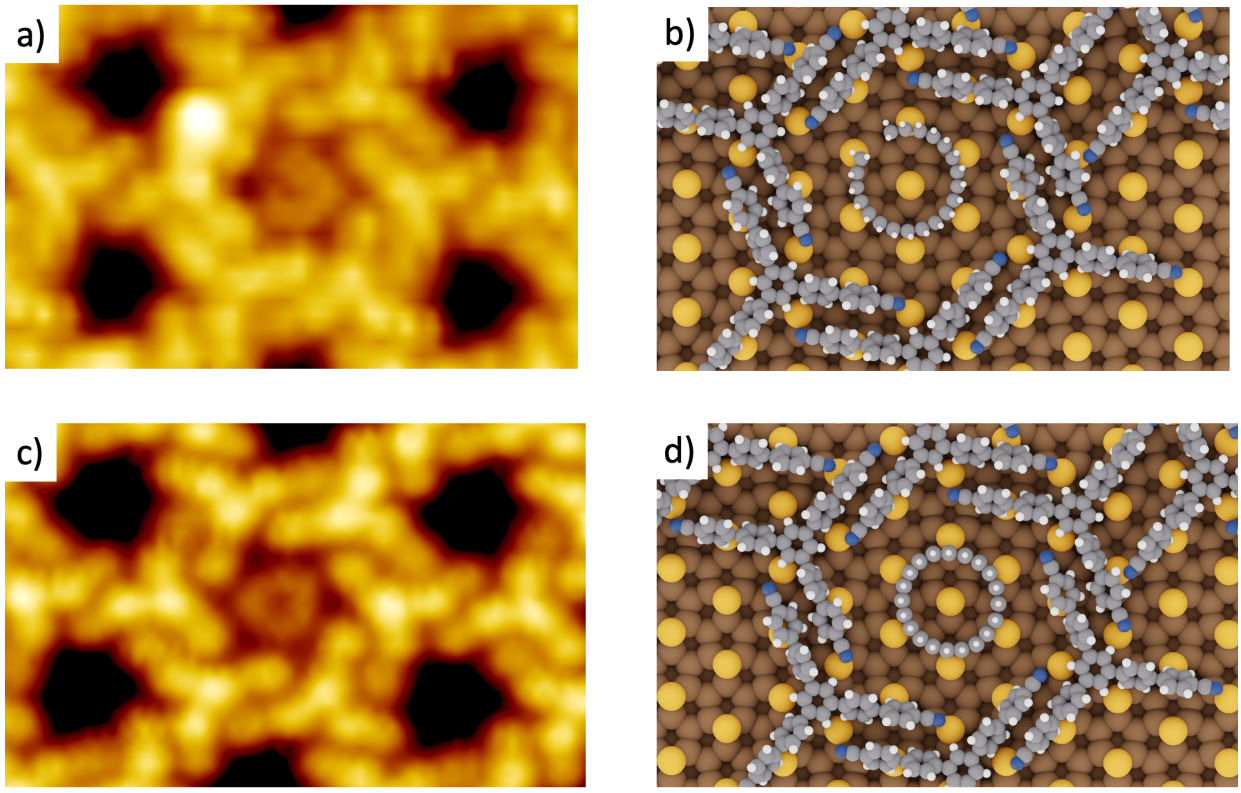

Figure 5. a) High-resolution STM image (8 nm x 5 nm, V_s = -2.5 V, I_t = 10 pA, T = 110 K) of a hexagonal nanopore of TCNBB supramolecular network on a Si(111)-B surface including an opened-ring structure. b) Proposed molecular model of the hexagonal filled nanopore shown in a). c) STM image (8 nm x 5 nm, V_s = -2.5 V, I_t = 10 pA, T = 110 K) of a closed-ring structure centered in an hexagonal nanopore. d) Proposed molecular model of c).

The opened- and closed ring-like structures observed in the hexagonal nanopores have the same length of 2.5 nm. Therefore, the opened-ring features can be attributed to a n-icosane ($C_{20}H_{42}$) molecule surrounding the central Si adatom of the hexagonal nanopore (Figure 5b and S4 in SI), and the closed-ring features to a cycloicosane molecule ($C_{20}H_{40}$) surrounding the central silicon

adatom of the hexagonal nanopore (Figure 5d and S4 in SI). In the two cases, icosane species are surrounding the central silicon adatoms of hexagonal nanopores of TCBNN supramolecular network. The presence of n-icosane and cycloicosane on the Si(111)-B surface should originate from the alkyl coupling of two different C_{10} species; one with one terminal radical (A) and one with two terminal radicals (B) (See Figure S5 in SI). In this case, A+A produces a n-icosane molecule, B+B gives cycloicosane, and A+B leads to a C_{20} chain with a terminal radical. This last species could establish a covalent bond with one of the peripherical Si adatom in the hexagonal nanopore, and finally gives a saturated opened-ring structure. As given the proportion of closed-ring structure observed with respect to opened-ring and grafted C_{10} alkyl chains, we can presume that the STM tip carry a similar proportion of C_{10} with two terminal radicals (B) than with only one (A).

DFT simulations

To clarify the origins of the supramolecular organization and the role of TCNBB/Si(111)-B network in stabilizing the two most abundant alkyl species observed in the two types of nanopores, we have investigated the structure and stability of adsorbed species with DFT calculations. First, the optimized unit cell used to study further alkyl adsorption on the TCNBB network on a Si(111)-B surface is reported at Figure 6. We are also showing a larger 2x2 unit cell to identify the location of the triangular and hexagonal nanopores within the TCNBB network. We considered the adsorption of three C_{10} alkyl chains in a triangular nanopore, and of one cycloicosane molecule centered on the more central Si adatom of a hexagonal nanopore. Finally, STM images of each resulting optimized geometry were simulated. The results are reported in Figure 7.

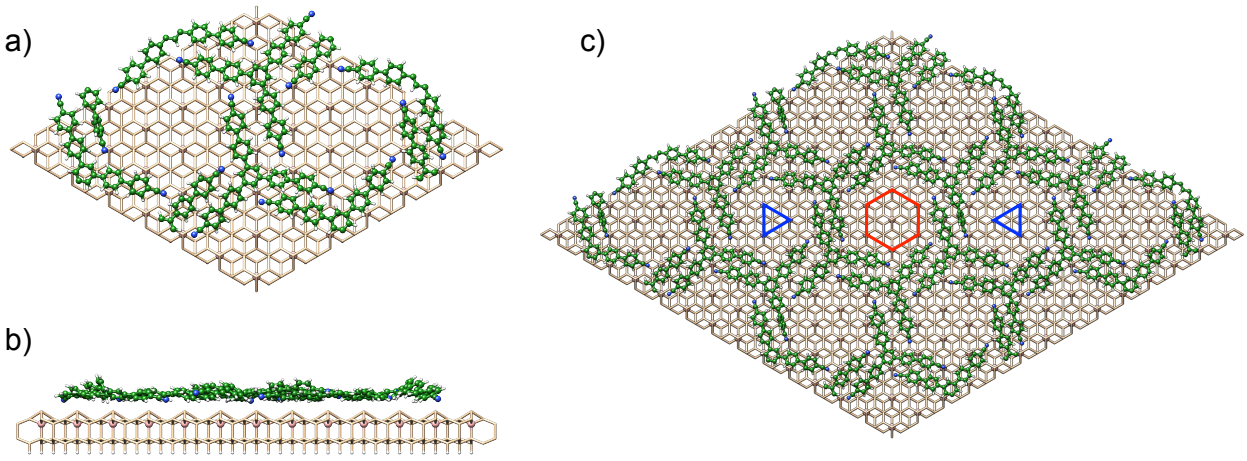

Figure 6. a) Top view and b) side view of the optimized unit cell used to model a TCNBB network on the Si(111)-B surface. c) A larger 2x2 view of the unit cell where the location of triangular (blue triangle) and hexagonal (red hexagon) is identified. The TCBNN network contains C (green), N (blue) and H (white) atoms, while the Si(111)-B substrate contains Si (light brown), B (pink) and H (white).

As reported in Table S1, the adsorption of TCNBB on Si(111)-B leads to the formation of a very stable network where the calculated adsorption energy contains the summation of cohesion energy of TCNBB molecules within the network and the interaction energy of TCNBB molecules with the substate. The molecular arrangement of TCNBB on Si(111)-B and the calculated STM image for that TCNBB network reported in Figure 7 are in very good agreement with the experimental STM image (Figures 7a and 7d). This also supports our specially developed methodology for the simulation of such large supramolecular networks adsorbed on the Si(111)-B surface.

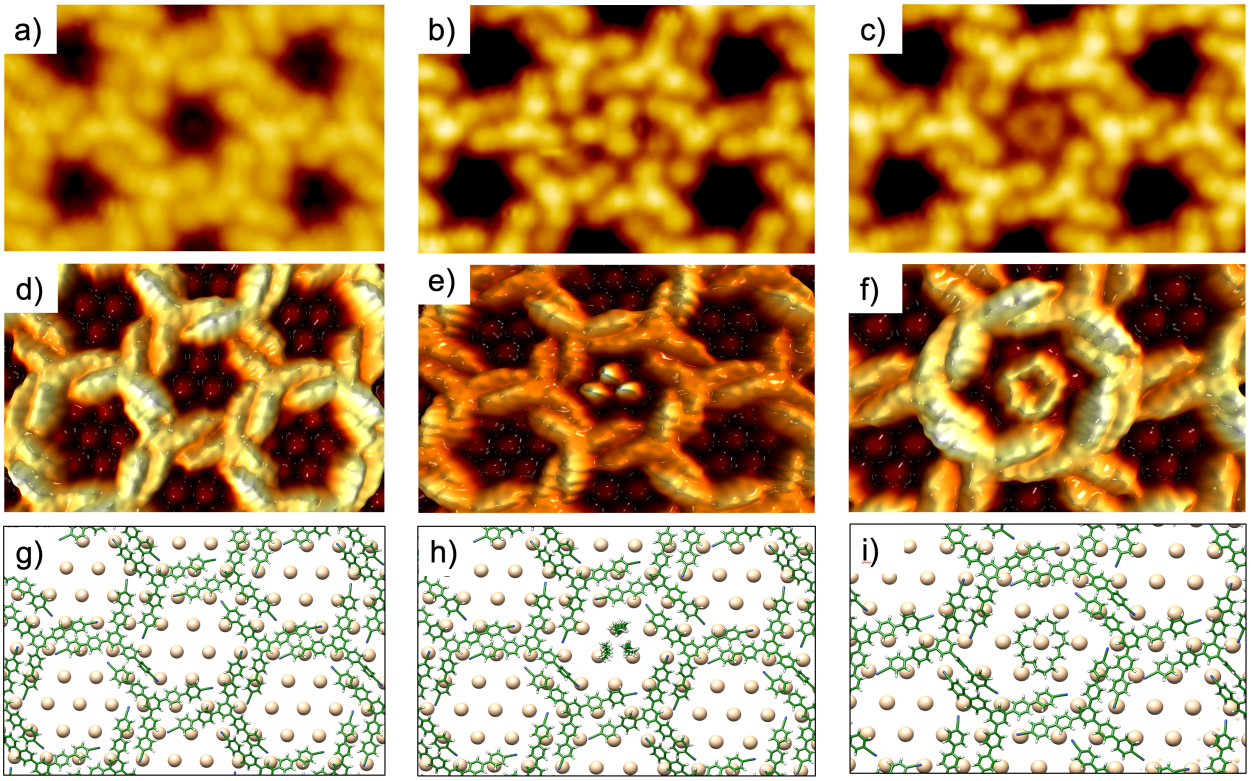

Figure 7. Comparison of experimental STM images (8 nm x 5 nm, V_s = -2.5 V, I_t = 10 pA, T = 110 K) of a TCNBB network on Si(111)-B substrate with a) empty nanopores, b) three C_{10} chains filling a triangular nanopore, and c) a C_{20} closed-ring confines in a hexagonal pore, to their respective simulated STM images (d-f), and associated molecular models (g-i). Only the topmost surface Si atoms are shown in the models for clarity.

The calculated adsorption energy (see Table S1) for three C_{10} chains (2.30 eV/C_{10} chain) on the available Si adatoms in the triangular nanopore is a summation of attractive chain-chain interactions energy and Si_{ad}-C_{10} bond energy formation. However, due to those weak lateral interactions, the upward C_{10} chains are quite flexible and their relative orientation in the nanopore may easily vary. As a result, the simulated STM image (Figure 7e) remains in very good agreement

with the experiments although the C_{10} chains appear less twisted with respect to the Si adatoms than in the experimental image (Figure 7b). We want to emphasize that we only observed the grafting of three C_{10} alkyl chains on the available Si adatoms within triangular nanopores, we never observe a partially filled triangular nanopore with one or two C_{10} alkyl chains. Hence, this experimental observation agrees with the DFT results, lateral interactions between three C_{10} alkyl chains in a triangular nanopore contribute to the overall stability of the triad. Surprisingly, no grafted C_{10} alkyl chain on Si adatoms among a hexagonal nanopore was observed. This is probably due to a more important steric hindrance for creating a C_{10} triad within a hexagonal nanopore since TCNBB molecules are closer to peripherical Si adatoms than in a triangular nanopore (See Figure S6 in SI).

For the presence of ring-like nanostructures into hexagonal nanopores, we considered the adsorption of cycloicosane to evaluate its stability. A calculated adsorption energy of 3.32 eV (See Table S1) sounds high for a physisorbed state but when divided by the number of C atoms in the chain, it gives a value (0.20 eV/C atoms) in the range of small physisorbed species. This significant adsorption energy could also explain why confinement of cycloicosane in hexagon nanopores is more frequently observed (3.4%) than the adsorption of three C_{10} chains in triangular nanopores (0.9%). Finally, the corresponding simulated STM image (Figure 7f) is in excellent agreement with the experimental image (Figure 7c). Furthermore, the formation of cycloicosane was observed although this necessitates overcoming a significant amount of deformation energy, hence we are confident that adsorbed opened-ring species should be as stable on Si(111)-B surface as cycloicosane.

Electronic considerations of the grafting of C_{10} alkyl chains on Si adatom

The formation of a covalent Si-C bond upon the grafting of an alkyl C_{10} chain on a low reactive Si(111)-B surface is a quite unusual process. Hence, we have explored the electronic modification of the underlying Si(111)-B surface induced by the grafting of the C_{10} alkyl chains on the Si adatoms in the triangular nanopore. The projected density of states (PDOS) of Si adatoms and B atoms just under Si adatoms forming or not a bond with a C_{10} chain are presented in Figure 8. The electronic states of Si adatoms (B atoms) involved in the Si-C bond are clearly shifted toward the Fermi level of the system. This is consistent with the covalent grafting of the C_{10} radicals with Si adatoms due to the interaction between empty states of the Si surface and filled states of the alkyl radicals. In addition, B atoms underneath Si adatoms are also participating in the grafting of C_{10} radicals. We observed hybridization of Si and B states at Fermi level, and an accumulation of charge density on B atom (Figure S7 in SI) when a C_{10} radical is grafted on a Si adatom, demonstrating its participation to the formation of the Si-C covalent bond.

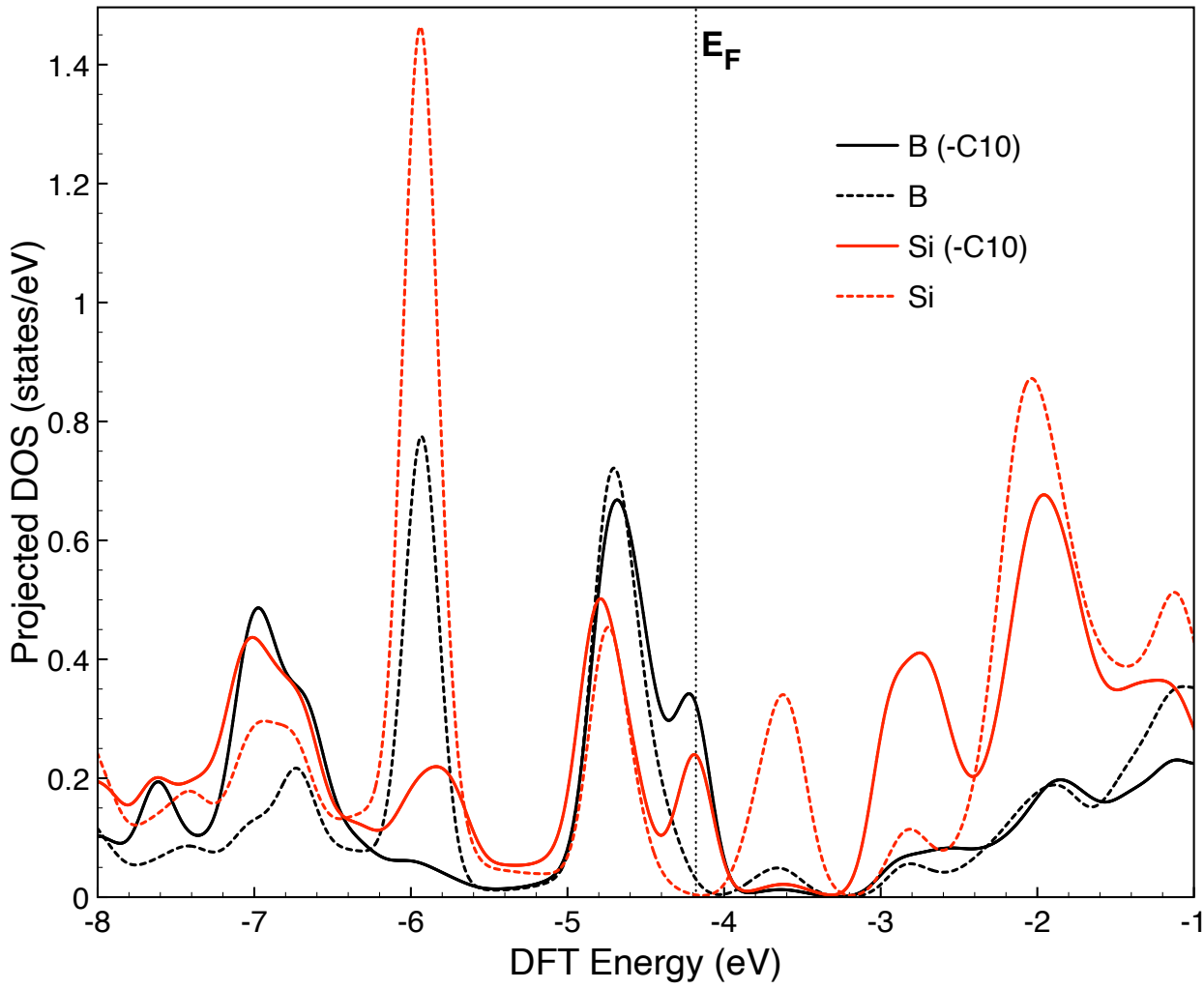

Figure 8. Projected density of states of B atoms and Si adatom from the Si(111)-B substrate involved (full lines) or not involved (dashed lines) in the formation of a covalent Si-C bond with C_{10} alkyl chains. The grafting of C_{10} alkyl chains leads to the shift of the first empty state of Si and B atoms below the Fermi level (E_F) of the complete system.

CONCLUSION

To summarize, we have combined experimental and theoretical efforts to demonstrate the ability of a STM tip to be used as a double efficient tool in on-surface synthesis. The STM tip can be used as a stimulus to induce a chemical reaction by adding electrons in a molecule with an atomic precision and then to convey, even on another substrate, some reactive alkyl radicals onto a specific area of an organic supramolecular adlayer. This double role of the STM tip completes its widely-used intrinsic ability to image molecules with a submolecular resolution in UHV by means of tunneling microscopy. In addition, we have also demonstrated that the reactivity of the resulting alkyl radicals on a hybrid organic/silicon surface can be tuned by the size of the nanopores of the organic adlayer. The generated and conveyed alkyl radicals aim at molecule-molecule dimerization or molecule-surface grafting, depending on the 2D confinement inside each nanopore. Finally, we demonstrate that boron atoms of the underlying surface are involved in the grafting of alkyl radicals with Si adatom of the surface. This new strategy is very efficient, and it could be used as a new opportunity to provide multi-functional nanostructures.

Supporting Information. The following files are available free of charge (pdf, including additional STM images of clean Si(111)-B surface, starting supramolecular network and additional simulations).

AUTHOR INFORMATION

Corresponding Author

*Frederic CHERIOUX, e-mail: frederic.cherioux@femto-st.fr

Author Contributions

FC synthesized the molecules. EG, JJ, and FP performed all STM experiments. AR performed DFT simulations. EG, FP, AR, and FC wrote the manuscript. All authors have read and agreed to the published version of the manuscript.

Funding Sources

This research was funded by Agence Nationale de la Recherche, grant number OVATION ANR-19-CE09-0020 and the Pays de Montbéliard Agglomération. A.R. acknowledges the support from the Natural Sciences and Engineering Research Council of Canada (NSERC), and he is grateful to Calcul Québec and the Alliance for providing computational resources.

ACKNOWLEDGMENT

We thank Pr. Dr. C. M. Thomas (IRCP, Paris, France) for fruitful discussions.

TOC Graphic

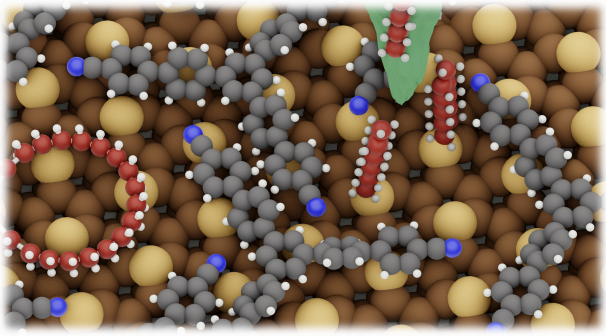

REFERENCES

[1] Grill, L.; Hecht, S. Covalent on-surface polymerization. *Nature Chem.* **2020**, *12*, 115.
[2] Clair, S.; de Oteyza, D. G. Controlling a chemical coupling reaction on a surface: tools and strategies for on-surface synthesis. *Chem. Rev.* **2019**, *119*, 4717.
[3] Shen, Q.; Gao, H.-Y.; Fuchs, H. Frontiers of on-surface synthesis: from principles to applications. *Nano Today* **2017**, *13*, 77.
[4] Lackinger, M. On-surface polymerization - a versatile synthetic route to two-dimensional polymers: On-surface polymerization. *Polym. Inter.* **2015**, *64*, 1073.
[5] Cai, J.; Ruffieux, P.; Jaafar, R.; Bieri, M.; Braun, T.; Blankeburg, S.; Muoth, M.; Seitsonen, A. P.; Saleh, M.; Feng, X.; Mullen K.; R. Fasel. Atomically precise bottom-up fabrication of graphene nanoribbons. *Nature* **2010**, *466*, 470.
[6] Para, F.; Bocquet, F.; Nony, L.; Loppacher, C.; Féron, M.; Chérioux, F.; Gao, D. Z.; Federici Canova, F.; Watkins, M. B. Micrometre-long covalent organic fibres by photoinitiated chain-growth radical polymerization on an alkali-halide surface. *Nature Chem.* **2018**, *10*, 1112.
[7] Li, J.; Merino-Diez, N.; Carbonell-Sanroma, E.; Vilas-Varela, M.; De Oteyza, D. G.; Pena, D.; Corso, M.; Pascual, J. I. Survival of spin state in magnetic porphyrins contacted by graphene nanoribbons. *Sci. Adv.* **2018**, *4*, eaaq0582.
[8] Kudernac, T.; Lei, S; Elemans, J. A. A. W.; De Feyter, S. Molecular and Supramolecular Networks on Surfaces: From Two-Dimensional Crystal Engineering to Reactivity. *Angew. Chem. Int. Ed.* **2009**, *38*, 402.
[9] Sosas-Vargas, L.; Eunkyoung, K.; Attias, A.-J. Beyond "decorative" 2D supramolecular self-assembly: strategies towards functional surfaces for nanotechnology. *Mater. Horiz.* **2017**, *4*, 570.
[10] Amrous, A.; Bocquet, F.; Nony, L. ; Para, F.; Loppacher, C.; Lamare, S.; Palmino, F.; Chérioux, F.; Gao, D. Z.; Canova, F. F.; Watkins M. B. Shluger, A. L. Molecular Design and Control Over the Morphology of Self-Assembled Films on Ionic Substrates. *Adv. Mater. Interfaces*, **2014**, *1*, 1400414.
[11] Zhang, H.-M.; Xie, Z.-X.; Mao, B.-W.; Xin Xu, X. Self-Assembly of Normal Alkanes on the Au (111) Surfaces.
Chem Eur. J. **2004**, *10*, 1415.
[12] Harikumar, K. R.; Polanyi, J. C.; Sloan, P. A.; Ayissi, S.; Hofer, W. A. Electronic Switching of Single Silicon Atoms by Molecular Field Effects. *J. Am. Chem. Soc.* **2006**, *128*, 12791.
[13] Zhong, D.; Franke, J.-H.; Podiyanachari, S. K.; Blomker, T.; Zhang, H.. Kehr, G.; Erker, G.; Fuchs, H.; Chi L. Linear Alkane Polymerization on a Gold Surface. *Science* **2011**, *334*, 213.
[14] Kinikar, A.; Di Giovannantonio, M.; Urgel, J. I.; Eimre, K.; Qiu, Z.; Gu, Y.; Jin, E.; Narita, A.; Wang, X.-Y.; Müllen, K.; Ruffieux, P.; Pignedoli, C. A.; Fasel, F. On-surface polyarylene synthesis by cycloaromatization of isopropyl substituents. *Nature Synth.* **2022**, *1*, 289.
[15] Grossmann L.; King, B. T.; Reichlmaier, S.; Hartmann, N.; Rosen, J.; Heckl, W. M. Björk, J.; Lackinger, M. On-surface photopolymerization of two-dimensional polymers ordered on the mesoscale. *Nature Chem.* **2021**, *13*, 730.
[16] Geagea, E.; Jeannoutot, J.; Féron, M.; Palmino, F.; Thomas, C. M.; Rochefort, A.; Chérioux, F. Collective radical oligomerisation induced by an STM tip on a silicon surface. *Nanoscale* **2021**, *13*, 349.

[17] Jacobse, P. H.; van der Hoogenband, A.; Moret, M.-E.; Gebbink, R. J. M.; Swart, I. Aryl radical geometry determines nanographene formation on Au(111). *Angew. Chem. Int. Ed.* **2016**, *55*, 13052.

[18] Zint, S.; Ebeling, D.; Schlöder, T.; Ahles, S.; Mollenhauer, D.; Wegner, H. A.; Schirmeisen, A. Imaging successive intermediate states of the on-surface Ullmann reaction on Cu(111): Role of the metal coordination. *ACS Nano* **2017**, *111*, 4183.

[19] Hla, S.-W.; Bartels, L.; Meyer, G.; Rieder, K.-H. Inducing All Steps of a Chemical Reaction with the Scanning Tunneling Microscope Tip: Towards Single Molecule Engineering. *Phys. Rev. Lett.* **2000**, *85*, 2777.

[20] Okawa, Y.; Aono, M. Materials science: Nanoscale control of chain polymerization. *Nature* **2000**, *409*, 683.

[21] Copie, G.; Cléri, F.; Makoudi, Y.; Krzeminski, C.; Berthe, M.; Chérioux, F.; Palmino, F.; Grandidier, B. Surface-Induced Optimal Packing of Two-Dimensional Molecular Networks. *Phys. Rev. Lett.* **2015**, *114*, 066101.

[22] Lyo, I.-W.; Kaxiras, E.; Avouris, Ph. Adsorption of Boron on Si(111): Its Effect on Surface Electronic States and Reconstruction. *Phys. Rev. Lett.* **1989**, *63*, 1261.

[23] Soler, J. M.; Artacho, E.; Gale, J. D.; García, A.; Junquera, J.; Ordejón, P.; Sánchez-Portal, D. The SIESTA method for ab initio order-N materials simulation. *J. Phys.: Condens. Matter* **2002**, *14*, 2745.

[24] García, A.; Papior, N.; Akhtar, A.; Artacho, E.; Blum, V.; Bosoni, E.; Brandimarte, P.; Brandbyge, M.; Cerda, J. I., Corsetti, F.; Cuadrado, R. Dikan, V.; Ferrer, J.; Gale, J.; Garcia-Fernandez, P.; Garcia-Suarez, V. M.; Garcia, S. ; Huhs, G. ; Illera, S. ; Korytar, R. ; Koval, P. ; Lebedeva, I. ;Lin, L. ;Lopez-Tarifa, P. ; Mayo, S. G. ; Mohr, S.; Ordejon, P.; Postnikov, A.; Pouillon, Y.; Pruneda, M.; Robles, R.. Sanchez-Portal, D.; Soler, J. M.; Ullah, R.; Yu, W. W.-Z., Junquera, J. Siesta: Recent developments and applications. *J. Chem. Phys.* **2020**, *152*, 204108.

[25] Lee, K.; Murray, E.; Kong, L.; Lundqvist, B. I.; Langreth, D. C. Higher-accuracy van der Waals density functional. *Phys. Rev. B* **2010**, *82*, 081101.

[26] Tang, W.; Sanville, E.; Henkelman, G. A grid-based Bader analysis algorithm without lattice bias. *J. Phys.: Condens. Matter* **2009**, *21*, 084204.

[27] Tersoff J.; Hamann, D. R. Theory of the scanning tunneling microscope. *Phys. Rev. B* **1985**, 31, 805.

[28] Makoudi, Y.; Jeannoutot, J.; Palmino, F.; Chérioux, F.; Copie, G.; Krzeminski, C.; Cleri, F.; Grandidier, B. Supramolecular Self-Assembly on the B-Si(111)-($\sqrt{3}$x$\sqrt{3}$) R30° Surface: From Single Molecules to Multicomponent Networks. *Surf. Sci. Rep.* **2017**, *72*, 316.

[29] Testaferri, L.; Tiecco, M.; Tingoli, M.; Chianelli, D.; Montanucci, M. The Reactions of Unactivated Aryl Halides with Sodium Methoxide in HMPA. Synthesis of Phenols, Anisoles, and Methoxyphenols. *Tetrahedron* **1983**, *39*, 193.

[30] Koppang, M. D.; Woolsey, N. F.; Bartak, D. E. Carbon-Oxygen Bond Cleavage Reactions by Electron Transfer. 2. Electrochemical Formation and Dimerization Reaction Pathways of Cyanodiphenyl Ether Radical Anions. *J. Am. Chem. Soc.* **1985**, 107, 4692.

[31] Baris, B.; Luzet, V.; Duverger, E.; Sonnet, P.; Palmino, F.; Cherioux, F. Robust and Open Tailored Supramolecular Networks Controlled by the Template Effect of a Silicon Surface. *Angew. Chem. Int. Ed.* **2011**, *50*, 4094.

[32] Makoudi, Y.; Beyer, M.; Lamare, S.; Jeannoutot, J.; Palmino, F.; Chérioux, F. Towards 1D nanolines on a monolayered supramolecular network adsorbed on a silicon surface. *Nanoscale* **2016**, *8*, 12347.

[33] Custovic, I.; Teyssieux, D.; Jeannoutot, J.; Lamare, S.; Palmino, F.; Abbasian, H.; Rochefort, A.; Chérioux, F.; Large-extended 2D supramolecular network of dipoles with parallel arrangement on a Si(111)–B surface. *Nanoscale* **2020**, *12*, 17399.
[34] Baris. B.; Jeannoutot, J.; Luzet, V.; Palmino, A.; Rochefort, A.; Chérioux, F. Noncovalent Bicomponent Self-Assemblies on a Silicon Surface. *ACS Nano* **2012**, *6*, 6905.
[35] Pavlova, T. V.; Kovalenko, S. L.; Eltsov, K. N. Room-Temperature Propylene Dehydrogenation and Linear Atomic Chain Formation on Ni(111*). J. Phys. Chem. C* **2020**, *124*, 8218.